

## Article

# Research on the Influence of Moisture Exchange between Oil and Cellulose on the Electrical Parameters of the Insulating Oil in Power Transformers

Konrad Kierczynski <sup>1,\*</sup>, Przemyslaw Rogalski <sup>1</sup>, Vitalii Bondariev <sup>1</sup>, Paweł Okal <sup>1</sup> and Daniel Korenciak <sup>2</sup>

<sup>1</sup> Department of Electrical Devices and High Voltage Technology, Faculty of Electrical Engineering and Computer Science, Lublin University of Technology, 38A, Nadbystrzycka Str., 20-618 Lublin, Poland

<sup>2</sup> Department of Measurement and Application Electrical Engineering, University of Zilina, 8215/1 Univerzitná, 01026 Zilina, Slovakia

\* Correspondence: k.kierczynski@pollub.pl; Tel.: +48-81-538-43-28

**Abstract:** The article presents an oil moistening method, identical to the oil moistening in power transformers. Moistening took place through the migration of moisture from the moistened pressboard to the brand new oil. The AC electrical parameters (admittance, phase shift angle, permittivity, loss tangent and conductivity) of the brand new and moistened insulating oil were tested. All measured parameters were found to be affected by the oil moistening. The greatest changes were observed in the loss tangent and conductivity. Moisturization increases the value of  $\tan\delta$  at a frequency of  $10^{-4}$  Hz from about 20 to about 70. With an increase in frequency to about 400–1000 Hz, a minimum is observed, the position of which depends on the temperature. Its value for moistened oil is about six times lower than for brand new oil. This moisturizing increased the activation energy of the conductivity from  $0.466 \pm 0.0265$  eV to  $0.890 \pm 0.0115$  eV. This is likely due to the acceleration of water molecules diffusion from the pressboard into the oil with increasing temperatures. The observed changes in the oil parameters caused by moistening should be taken into account while analyzing the power transformers insulation condition using the FDS method.

**Keywords:** transformer diagnostics; FDS method; insulation of transformers; moisture; mineral oil; cellulose; pressboard



**Citation:** Kierczynski, K.; Rogalski, P.; Bondariev, V.; Okal, P.; Korenciak, D.

Research on the Influence of Moisture Exchange between Oil and Cellulose on the Electrical Parameters of the Insulating Oil in Power Transformers. *Energies* **2022**, *15*, 7681. <https://doi.org/10.3390/en15207681>

Academic Editor: Zbigniew Nadolny

Received: 21 September 2022

Accepted: 17 October 2022

Published: 18 October 2022

**Publisher's Note:** MDPI stays neutral with regard to jurisdictional claims in published maps and institutional affiliations.



**Copyright:** © 2022 by the authors. Licensee MDPI, Basel, Switzerland. This article is an open access article distributed under the terms and conditions of the Creative Commons Attribution (CC BY) license (<https://creativecommons.org/licenses/by/4.0/>).

## 1. Introduction

One of the basic elements of the power transformer is the insulation system. The operational reliability of transformers and their service lives is largely determined by the quality of the electrical insulation. Currently, most cellulose materials and petroleum-based mineral oils are used for the production of transformers electrical insulation [1–4]. After completion, the transformer is hermetically sealed. Then, a vacuum drying of the insulation is performed. Before mineral oil is poured into the transformer tank, it is treated to reduce the moisture level to about 3–7 ppm and for removing dissolved gases [5–8]. Then, also under vacuum, the transformer is filled with heated oil. This improves the insulating properties of the system, accelerates the impregnation of cellulose with oil and removes gas bubbles, which are the source of partial discharges [9–11]. After these operations, the moisture level of cellulose in the transformer insulation does not exceed 0.8% by weight. Power transformers are designed to operate for at least 25 years. Due to many years of transformer operations (25 and more years), the moisture content of cellulose may increase to 5% by weight and even higher. The moisture increase usually takes place as follows. Moisture enters the transformer tank and then dissolves into the oil. The oil movement, caused by convection or forced circulation, causes the water molecules to be delivered to the cellulose, where they are absorbed. This is due to the fact that the solubility of water in cellulose is about 1000 times greater than in insulating oil [12]. The value of 5%

by weight is, in a sense, the critical value. Exceeding this value may lead to transformer failure [13–15]. Diagnostic methods, often based on nondestructive electrical methods, are used to determine the moisture level and other possible insulation defects that may arise over many years of operation. They are: Return Voltage Measurement (RVM) [16–18], Polarization Depolarization Current (PDC) [19–21] and Frequency Domain Spectroscopy (FDS) [22–24]. The FDS method is currently considered to be the most effective. The meters used in measurements with this method make it possible to determine the electrical parameters of the insulation. Their software can estimate the moisture level of cellulose. In the works [25,26], it was established that the cellulose moisture levels estimated by using FDS meters differ from the actual ones. This may be a result from the use of conductivity and dielectric relaxation models that do not accurately describe the processes occurring in cellulose–oil insulation. The models often used to analyze the FDS measurement results are: Debye's [27], Cole-Cole [28,29], Dawidson-Cole [30,31] and Havriliak-Nagami [32]. These models assume that, when the frequency tends toward zero (constant voltage), the conductivity should also tend toward zero. This is inconsistent with all known test results for which the conductivity at ultra-low frequencies is a constant value. It was also found that, for a moist pressboard impregnated with insulating oil, in the ultra-low frequency region, the DC (Direct Current) and AC (Alternating Current) conductivity values are equal [33]. The correct determination of the cellulose moisture level in transformers can only be achieved with the use of a physical model that faithfully describes the processes of conduction and dielectric relaxation occurring in the insulation.

Pressboard, impregnated with oil, is a two-phase composite material. Moistening of the pressboard causes the composite to become a three-phase one. Measurements of the DC conductivity dependence on the water content showed that the conductivity of the composite is caused by the presence of water. Conduction in the composite is determined by the quantum mechanical phenomenon of electron tunneling between water molecules. In the works [34,35], to analyze the AC conductivity dependence on the moisture content, the DC and AC conductivity model, determined by the quantum mechanical phenomenon of electron tunneling between potential wells with nanometer dimensions proposed in publications [36–38], was used. This model has been experimentally verified for semiconductors [39] and nanocomposites [40–43]. Based on the analysis performed in the works [34,35], it was found that water is present in the oil-impregnated pressboard in the form of nanodrops with a diameter of about 2.2 nm. Each nanodrop contains, on average, approximately 200 water molecules. In such a system, tunneling of the electron takes place from one nanodrop to the other. As a result of tunneling, an electric current flow and electric dipole creation occurs. This causes additional polarization of the material [44–46]. After the relaxation time has elapsed, the electric field of the positively charged nanodrop causes the electron to return to the nanodrop from which it started tunneling. This leads to the dipole vanishing. The value of the relaxation time depends on the average distance between the nanodrops and the temperature [34].

Usually, in the FDS method, the diagnosis of insulation by the frequency analysis of the loss tangent is used; see, for example, [47,48].

As is known, the transformer insulation system is a complex cylindrical system consisting of barriers, spacers and oil channels. CIGRE in publication [49] proposed a simplified model of transformer insulation. It is a series parallel flat capacitor system with two parameters describing the geometry of the insulation system. Parameter X describes the contribution of the barriers in the insulation system geometry. Parameter Y describes the contribution of the spacers in the insulation system geometry. Application of the XY CIGRE model significantly simplifies the analysis of transformer insulation diagnostic results based on the loss tangent measurements. The value of the loss tangent in the CIGRE model is influenced by both the parameters of the moist oil-impregnated pressboard (barriers and spacers) and the parameters of the mineral oil (oil channels). This is most important when the moisture content reaches a limit of about 5% by weight, which may result in the failure of the transformer. The electrical properties of the oil-impregnated pressboard,

moistened in a manner identical to the moisturization process in transformers, due to a moisture content of  $5 \pm 0.2\%$  by weight was examined in the works [26,33,46].

The XY system was investigated in [26], in which the barriers and spacers were made with pressboard plates with a moisture content of  $5 \pm 0.2\%$  by weight. The oil channel was filled with factory new mineral insulating oil. It was found that, in order to adjust the loss tangent waveforms for the system made according to CIGRE, the software of the FDS meter introduces gigantic, i.e., more than six orders of magnitude fluctuations of the oil conductivity during the transition from one measuring temperature to the next. Such large, abrupt changes in conductivity are rather impossible. This means that the matching algorithm used in the FDS meter inaccurately reflects the temperature dependence of the AC parameters of the oil.

As it is known [12], along with the increase of the moisture content in the pressboard, which is a part of the transformer insulation, the oil moisture also increases. Under the conditions of the thermodynamic equilibrium between the moisture in the oil and the pressboard, the moisture content of the oil is several orders lower than the moisture content of the pressboard. As the temperature of the transformer insulation increases, moisture diffuses from the cellulose into the oil, causing an increase of oil moisture content. The time needed to establish a thermodynamic equilibrium depends on the values of the initial and final temperatures. When the temperature is lowered, the process takes place in the opposite direction. Such changes in the moisture level may cause changes in the electrical parameters of the oil. This means that, for the correct determination of the cellulose component moisture content, by measuring the loss tangent of the power transformer insulation, one should take into account the changes in the electrical parameters of the insulating oil, which are related to the oil moisture content increase, caused by changes in the insulation temperature.

The aim of this work was to develop a method of oil moistening identical to the moisturization process in transformers and to measure the frequency and temperature dependencies of the basic electrical parameters of moistened oil. The obtained measurement results were compared with those for brand new oil in order to analyze the influence of moisture on the electrical parameters of the oil.

## 2. Materials and Methods

The alternating current flow in dielectrics is described by the second Maxwell equation [50]:

$$\Delta \times \vec{H} = \vec{j}_R + \vec{j}_C = \sigma(\omega) \vec{E}_0 \sin(\omega t) + \omega \cdot \epsilon'(\omega) \cdot \epsilon_0 \cdot \vec{E}_0 \sin\left(\omega t - \frac{\pi}{2}\right), \quad (1)$$

where:  $\vec{H}$ —magnetic field strength vector,  $\vec{j}_R$ —conduction current density,  $\vec{j}_C$ —displacement current density,  $E_0$ —electric field amplitude,  $\sigma(\omega)$ —conductivity,  $\epsilon'(\omega)$ —relative dielectric permittivity,  $\epsilon_0$ —vacuum dielectric permittivity,  $\omega = 2\pi f$ —circular frequency and  $f$ —frequency.

Equation (1) shows that the current flow in the dielectric is determined by two material parameters: conductivity and permittivity. Conductivity describes the ability of a material to conduct an electric current. Permittivity characterizes the polarization of the material. Formula (1) shows that the phase shift angle between the conduction current and the displacement current vectors is  $-90^\circ$ . This means that, in a real dielectric, the phase shift angle  $\phi$  takes values in range  $0^\circ \geq \phi \geq -90^\circ$ .

So-called impedance (admittance) meters are used to measure the AC properties of dielectrics. Determination of the transformer insulation parameters is performed with the use of dedicated meters called FDS (Frequency Domain Spectroscopy) meters. Admittance or FDS meters measure values of two basic parameters, which, in the case of dielectrics, are

the admittance  $Y$  and the phase shift angle  $\varphi$ . The admittance is equal to the quotient of the current amplitude and supply voltage amplitude [51]:

$$Y = \frac{I}{V}, \quad (2)$$

where:  $Y$ —admittance,  $V$ —supply voltage amplitude, and  $I$ —electric current amplitude.

The phase shift angle is equal to the difference of the angles at which instantaneous values of the current and voltage cross zero [51]:

$$\varphi = \varphi(i = 0) - \varphi(v = 0), \quad (3)$$

where:  $\varphi$ —phase shift angle,  $\varphi(i = 0)$ —the angle at which the instantaneous value of the current becomes zero and  $\varphi(v = 0)$ —the angle at which the instantaneous voltage value is zero.

Based on the admittance  $Y$  value and the phase shift angle  $\varphi$  in the equivalent parallel circuit, the conductance  $G_p$  and capacitance  $C_p$  are determined [51]:

$$G_p = |Y \cos \varphi|, \quad (4)$$

$$C_p = \frac{|Y \sin \varphi|}{\omega}, \quad (5)$$

In the study, a flat capacitor was used, in which the oil was poured between the voltage and measuring electrodes. Conduction and displacement currents flow between the two flat electrodes. A parallel equivalent circuit corresponds to this. The material parameters included in the second Maxwell equation—conductivity and permittivity—are calculated on the basis of the geometrical dimensions of the dielectric and the  $G_p$  and  $C_p$  values [52]:

$$\sigma = \frac{G_p d}{S} = \frac{Y |\cos \varphi| d}{S}, \quad (6)$$

where:  $\sigma$ —conductivity,  $G_p$ —conductance,  $d$ —oil layer thickness and  $S$ —measuring the electrode surface area.

$$\epsilon' = \frac{C_p d}{\epsilon_0 \cdot S} = \frac{Y |\sin \varphi| \cdot d}{\omega \cdot \epsilon_0 \cdot S}, \quad (7)$$

where:  $C_p$ —capacity,  $\epsilon_0$ —dielectric permittivity of vacuum,  $d$ —oil layer thickness,  $S$ —measuring electrode surface area and  $\omega$ —circular frequency.

To analyze the results of the transformer insulation tests, a number of publications [53–55] use the loss factor  $\epsilon''$ , otherwise known as the imaginary component of the complex permittivity:

$$\epsilon'' = \frac{\sigma}{\omega \epsilon_0}, \quad (8)$$

Substituting the conductivity value given by Formula (6) into Formula (8) shows:

$$\epsilon'' = \frac{Y |\cos \varphi| d}{\omega \epsilon_0 S}, \quad (9)$$

Formulas (6), (7) and (9) show that the geometrical dimensions of the dielectric are needed to determine the conductivity, permittivity and loss factor. These dimensions are easy to obtain in laboratory tests. However, in the measurements of industrial equipment, such as power transformers, especially those manufactured several decades ago, it may be difficult or even unattainable. Therefore, the loss tangent  $\tan \delta$  is often used to analyze the test results of the devices:

$$\tan \delta = \frac{I_R}{I_C} = \frac{\epsilon''}{\epsilon'} = \frac{\sigma}{\omega \epsilon' \epsilon_0}, \quad (10)$$

where:  $I_R$ —resistance component of the electric current and  $I_C$ —capacitive component of the electric current.

Substituting Formulas (7) and (9) into Formula (10), we find:

$$\tan \delta = \frac{Y |\cos \varphi|}{\mu \epsilon_0 S} = \frac{|\cos \varphi|}{|\sin \varphi|} = |\cot \varphi|, \quad (11)$$

As can be seen from Formula (11), the value of  $\tan \delta$  does not depend on the geometrical dimensions of the homogeneous material. To determine  $\tan \delta$ , it is enough to specify the phase shift angle  $\varphi$ .

Formulas (4)–(11) show that the values of conductance (resistance), capacitance, conductivity, permittivity, loss factor and loss tangent are functions of basic parameters, such as admittance and phase shift angle, determined by the admittance (impedance) meters.

In this work, the measuring system described in the works [25,46,56–58] was used for the tests. The electrical parameters of the oil were determined using the DIRANA meter—FDS-PDC dielectric response analyzer (OMICRON Energy Solutions GmbH, Berlin, Germany) [59]. The measurements were made in a thermostatic chamber at six measuring temperatures from 293.15 K to 333.15 K with steps of 8 K. The uncertainty of measuring and maintaining the temperature during the tests was not worse than  $\pm 0.01$  K. The frequency range of the Diran meter was from 0.0001 Hz to 5000 Hz. In the frequency range of 0.001 Hz–5000 Hz, the measurements were made at 10 points per decade, while, in the range of 0.0001 Hz–0.001 Hz, they were made at 6 points per decade. The measurement frequencies were chosen in such a way that, on the plot with double logarithmic coordinates, the measurement points were evenly distributed along the  $x$ -axis.

In order to test the dielectric properties of the oil, a measuring capacitor was used, the diagram of which is shown in Figure 1.

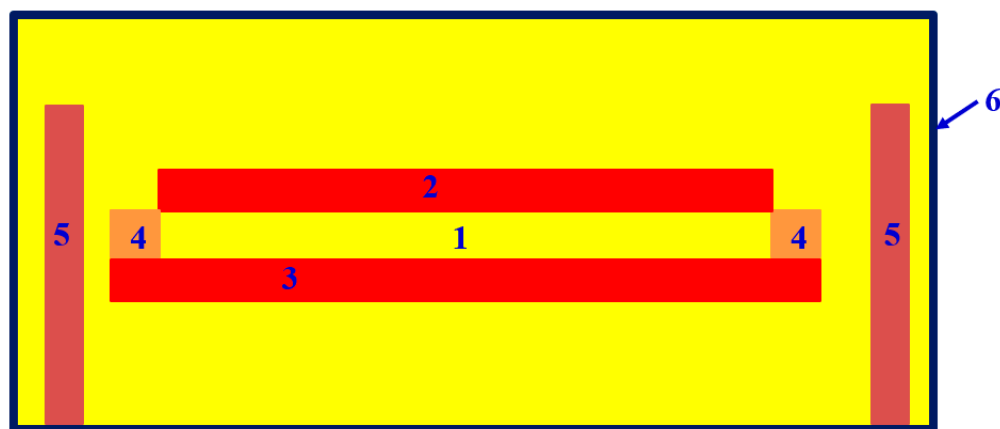


**Figure 1.** Diagram of the system for testing the insulating oil electrical properties. 1—mineral oil, 2—measuring electrode, 3—voltage electrode, 4—spacers (6 pieces), 5—moistened oil-impregnated pressboard placed in the vessel in the second series of tests and 6—hermetic vessel.

The upper part of the capacitor, which includes the measuring electrode, is separated from the voltage electrode by 6 spacers made of insulating material insoluble in oil. The capacitor was then placed in the glass vessel and filled with factory new insulating oil. After being sealed, the vessel was placed in a thermostatic chamber, and the first series of tests was carried out to measure the AC properties of brand new oil at six temperatures. Factory new mineral-insulating oil produced by the Nynas Company, intended for power transformers, was used in the tests. The moisture content of the oil did not exceed 5 ppm.

In order to investigate the influence of moisture on the oil electrical properties, a second series of tests was performed. This experiment accurately reflected the process of moisture exchange between the oil and pressboard, taking place in a highly moistened transformer. For this purpose, pressboard plates with a moisture content of  $5 \pm 0.2\%$  by wt.

were placed in a vessel with brand new oil (Figure 1). The volume of the pressboard was about 10 times smaller than the volume of the oil. Such a ratio of pressboard to oil is typical for power transformers with a voltage rating of 110 kV and more. After being sealed, the vessel was placed in a thermostatic chamber and left at a temperature of  $293.15 \pm 0.01$  K for about 100 h. During this period, moisture diffused from the moistened pressboard into the oil until reaching the thermodynamic equilibrium between the oil, water and pressboard, described by Formula (12). The new method of moistening the oil is fundamentally different from those known and described in the literature. It is obvious that the oil moisture in the method developed by us increases, as in the transformers, along with the temperature increase. This causes a temperature variation in the AC parameters, other than when testing the constant moisture oil, for example, taken from a transformer. Then, electrical tests were performed at the temperature of 293.15 K. After the tests were completed, the next temperature was set to 301.15 K, and after it was reached, the oil was left at this temperature for about 15 h. During this time, another thermodynamic equilibrium between the oil and the moistened pressboard was achieved with a higher moisture content in the oil. After the electrical measurements were made, the next temperatures were set, the capacitor with oil was heated in them for 15 h and subsequent measurements were made. In this way, the dependencies of admittance  $Y$ , phase shift angle  $\varphi$ , alternating current conductivity  $\sigma_{AC}$ , permittivity  $\epsilon'$  and loss tangent  $\tan\delta$  were obtained for brand new oil and for oil moistened by moisture migration from the pressboard.

### 3. Test Results and Analysis of Mineral Insulating Oil Electrical Properties

Figure 2 shows the admittance dependencies on the frequency and temperature, determined for a brand new insulating oil and for oil moistened in the same way as the oil moistening process in a power transformer with a high moisture content in cellulose. In the second case, the moisture diffused into the oil from pressboard moistened to 5% by weight. Such a moisture content in pressboard can be achieved after many years of a transformer operation.

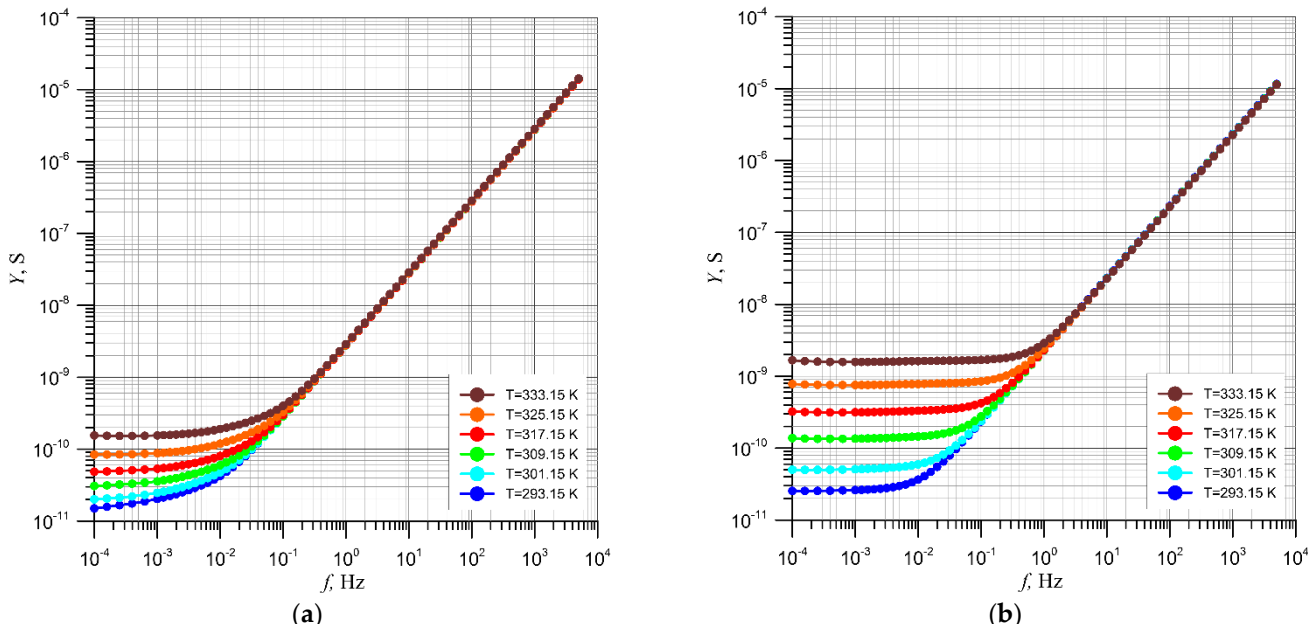


**Figure 2.** Frequency dependencies of the admittance of mineral insulating oil with a moisture content of 5 ppm—(a) and moistened mineral oil—(b) at temperatures from 293.15 K to 333.15 K in steps of 8 K.

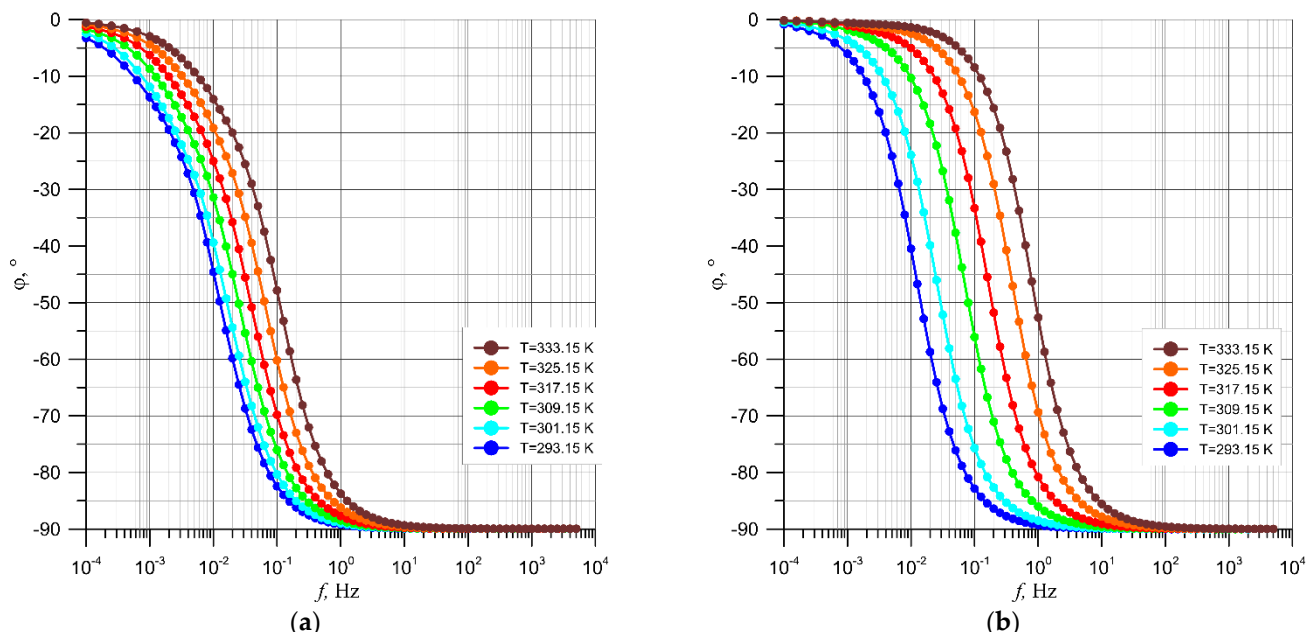
The comparison of admittance curves obtained for the brand new and moistened oil shows that oil moistening has a significant impact on the obtained dependencies. In both cases, admittance is practically frequency-independent in the low-frequency region. In this frequency region, however, there is a dependence of admittance on temperature. As the frequency increases, the admittance slowly increases. As it is known [33], the beginning of the admittance increase occurs close to the frequency defined by the dielectric relaxation time:

$$f = \frac{1}{2\pi\tau}, \quad (12)$$

where:  $f$ —admittance rise frequency and  $\tau$ —dielectric relaxation time of oil.

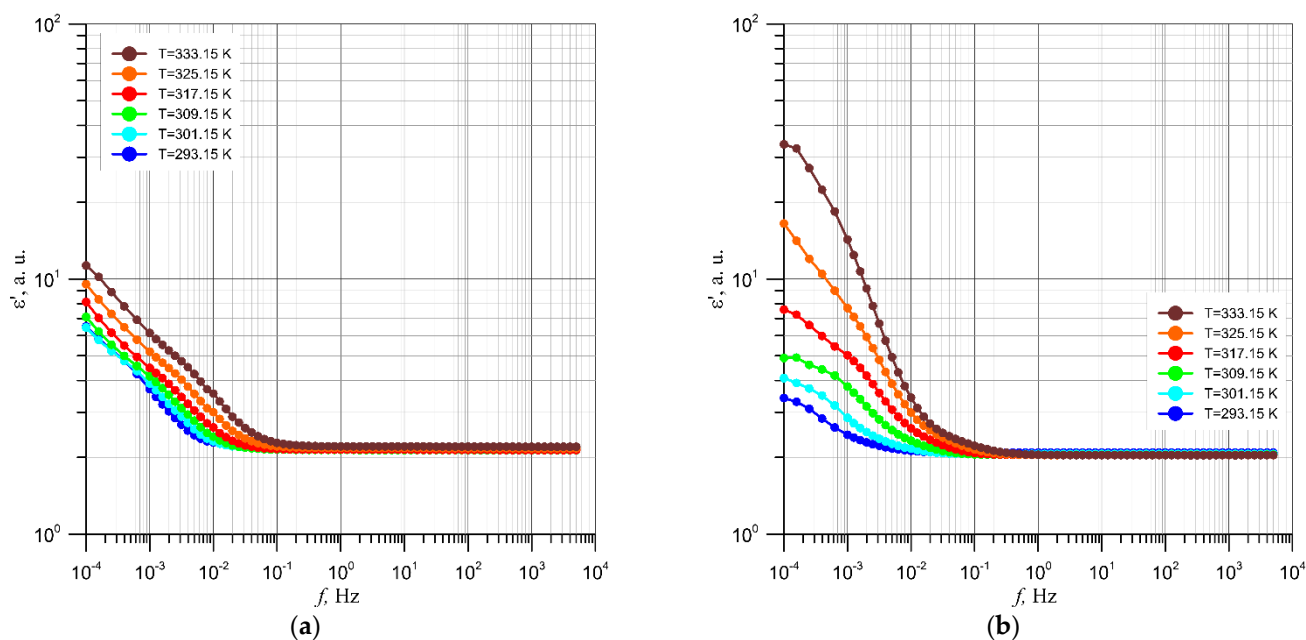
Then, the linear dependence of the admittance on frequency is observed. The temperature dependence of admittance disappears. Significant differences between the admittance values of brand new and moistened oil occur in the low-frequency area. First, in the case of a moistened oil, the length of the constant admittance value section is increased. This means that, according to Formula (12), in the case of a moistened oil, the dielectric relaxation time is lowered. The comparison of the plots in Figure 2a,b shows that the relaxation time of the moistened oil is about 10 times shorter than that of the brand new one. Secondly, as the temperature increases from 293.15 K to 333.15 K, the differences in the admittance values for the lowest frequency of  $10^{-4}$  Hz increase. For brand new oil, the values change about 10 times, and, for moistened oil, about 100 times. This means that the changes in both the dielectric relaxation time and the low-frequency admittance values are undoubtedly related to the moisturization of the oil.

Figure 3 shows the phase shift angle dependencies on frequency and temperature for the brand new oil and for the moistened oil. The comparison of the plots clearly shows that, in the case of the phase shift angle, oil moistening undoubtedly influences the obtained curves. Firstly, in the moistened oil, the length of the segment in which the values of the angle  $\phi$  are close to zero is lengthened. A value of  $\phi$  close to zero means that mainly resistive-type conduction occurs in this frequency region. Secondly, in the region of higher frequencies, the rate of the phase shift angle modulus rise increases. Thirdly, due to the decrease in the value of the dielectric relaxation time, the influence of temperature on the plots shift to the area of higher temperatures increases.



**Figure 3.** Frequency dependencies of the phase shift angle of mineral insulating oil with a moisture content of 5 ppm—(a) and moistened mineral oil—(b) at temperatures from 293.15 K to 333.15 K in steps of 8 K.

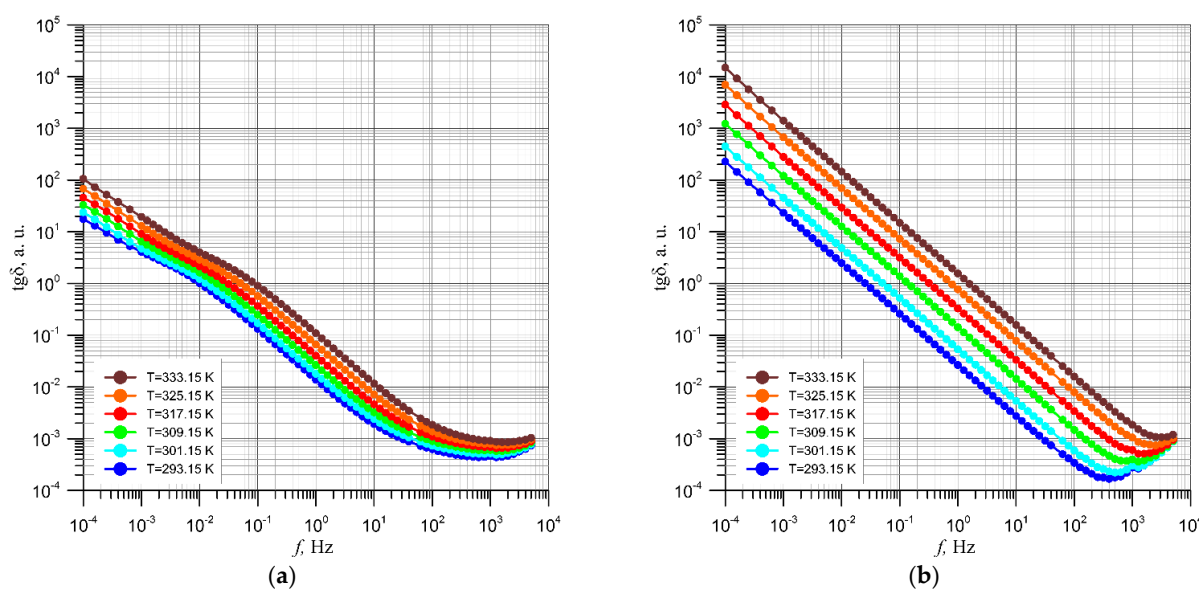
Figure 4 shows the dielectric permittivity dependence on frequency and temperature of brand new and moistened oil.



**Figure 4.** Frequency dependencies of the dielectric permittivity of mineral insulating oil with a moisture content of 5 ppm—(a) and moistened mineral oil—(b) at temperatures from 293.15 K to 333.15 K in steps of 8 K.

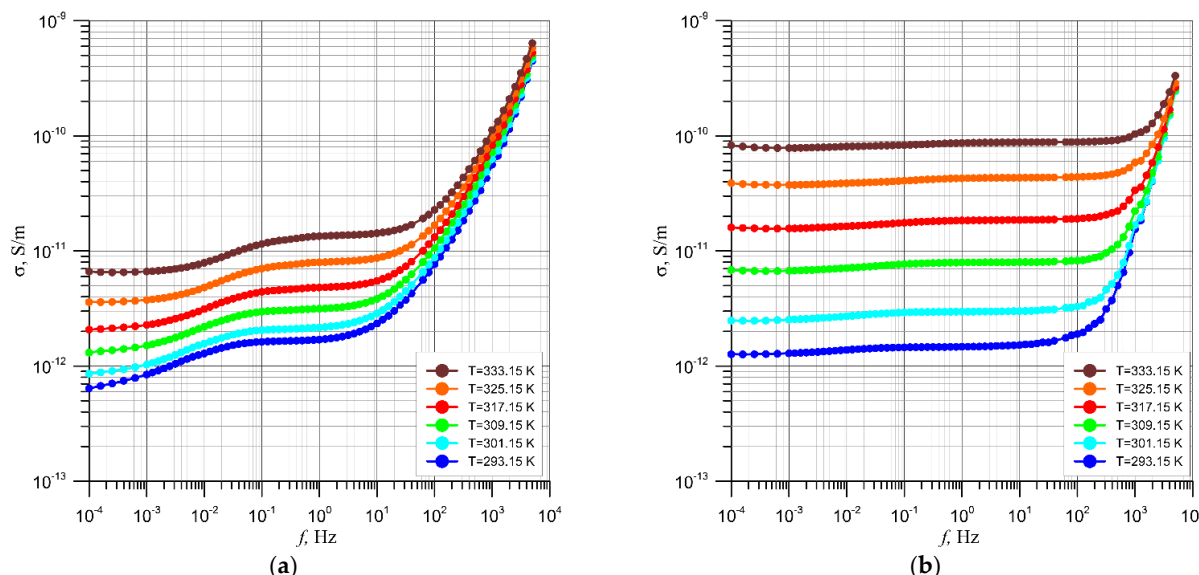
Figure 4a,b show that the permittivity of the oil in the frequency range above 0.1 Hz has a constant value of about 2.2. This is in line with the previously known results [60]. In the low-frequency area ( $f < 0.1$  Hz), as the frequency decreases, the permittivity of the brand new oil increases from about three to about five times, depending on the measuring temperature. Oil moisturization causes changes in the permittivity curves in this frequency range. At temperatures from 293.15 K to 333.15 K, there is a slight decrease in permittivity, not exceeding two times. The degree of permittivity reduction is greatest at 293.15 K, and it decreases with the increasing temperature. For temperatures above 333.15 K, the permittivity starts to increase compared to brand new oil. For the highest temperature of 333.15 K, the increase is about three times. The observed changes in permittivity are related to the increase in oil moisture with the increasing temperature.

Figure 5 shows the loss tangent dependence on the frequency and temperature of the brand new and moistened insulating oil. The figure shows that moisturization changes the shape of the curves. The plot for a brand new oil at a temperature of 293.15 K shows that, at a frequency of  $10^{-4}$  Hz, the value of the loss tangent is about 20. The increase in frequency causes a decrease in the value of  $\tan\delta$ . With the frequency increase above 0.01 Hz, the rate of the  $\tan\delta$  value reduction increases. In the frequency range above 10 Hz, the decrease of the plot slows down, and at a frequency of about 1000 Hz, the minimum is observed. The  $\tan\delta$  minimum value is about  $4 \times 10^{-4}$ . For a moistened oil at a frequency of  $10^{-4}$  Hz, the loss tangent value increases, compared to brand new oil, to about 70. In the range from  $10^{-4}$  Hz to about 0.01 Hz, the slope of the  $\tan\delta$  value reduction is greater than for brand new oil and continues in practically the same way up to a minimum at a frequency of about 400 Hz. The  $\tan\delta$  minimum value for the moistened oil is about six times lower than for the brand new one and is about  $6 \times 10^{-5}$ . Additionally, the shape of the minimum is very clear compared to the brand new oil. With the increase of the measuring temperature, the  $\tan\delta$  curves for the moistened oil shifts to the area of higher frequencies much faster than for the brand new oil. This phenomenon is related to the relaxation time reduction due to the increase in moisture.



**Figure 5.** Frequency dependencies of the loss tangent of mineral insulating oil with a moisture content of 5 pm—(a) and moistened mineral oil—(b) at temperatures from 293.15 K to 333.15 K in steps of 8 K.

The greatest changes were observed for conductivity dependencies on the frequency and temperature. Figure 6 shows the conductivity dependencies of brand new and moistened mineral-insulating oil. A flat section in the low-frequency area occurs in the conductivity plots of brand new oil. With a frequency increase, an approximately double increase in conductivity is observed, transition to a steady state and then a very rapid further increase. A temperature increase from 293.15 K to 333.15 K increases the conductivity by about 10 times. This means that, in brand new oil, at least two current conduction mechanisms occur. Oil moistening causes the disappearance of the first segment of the conductivity increase. In the second stage, the rate of conductivity increases. Oil moistening causes about 60 times greater changes in conductivity with the temperature increase compared to brand new oil.



**Figure 6.** Frequency dependencies of the conductivity of mineral-insulating oil with a moisture content of 5 ppm—(a) and moistened mineral oil—(b) at temperatures from 293.15 K to 333.15 K in steps of 8 K.

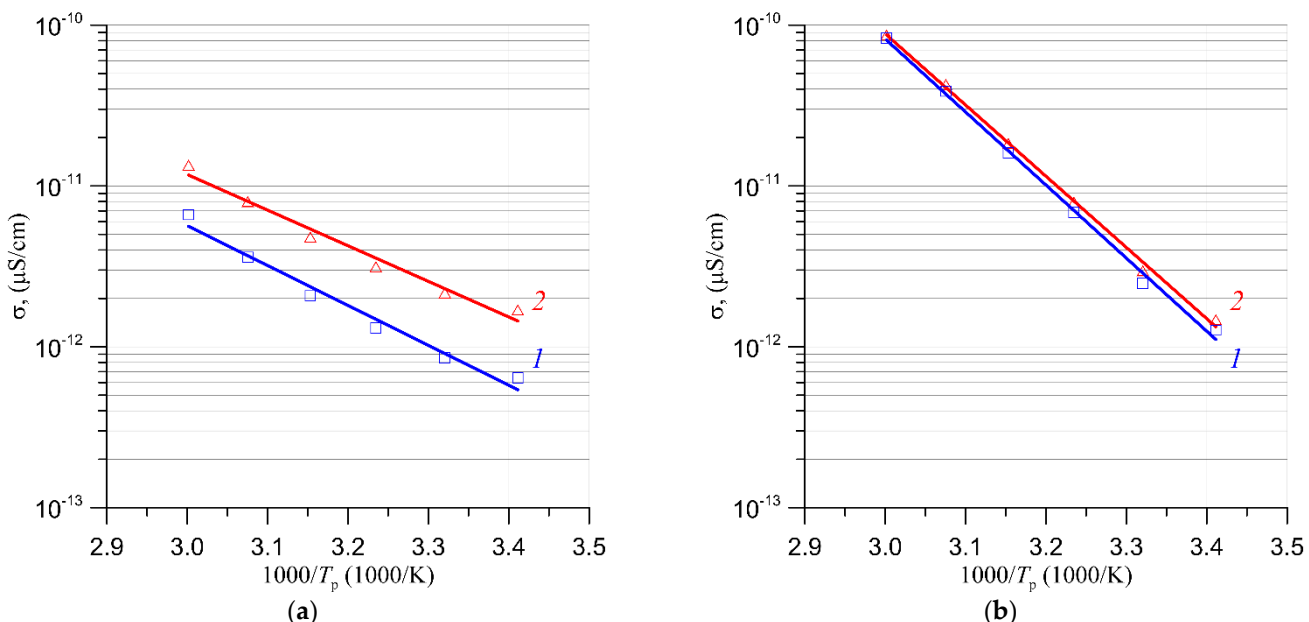
In insulating materials, the conductivity dependence on temperature is described by the formula [61]:

$$\sigma(T) = \sigma_0 \exp\left(-\frac{\Delta E_\sigma}{kT}\right), \quad (13)$$

where:  $\sigma(T)$ —conductivity,  $\sigma_0$ —numerical factor,  $\Delta E_\sigma$ —conductivity activation energy,  $k$ —Boltzmann's constant and  $T$ —temperature.

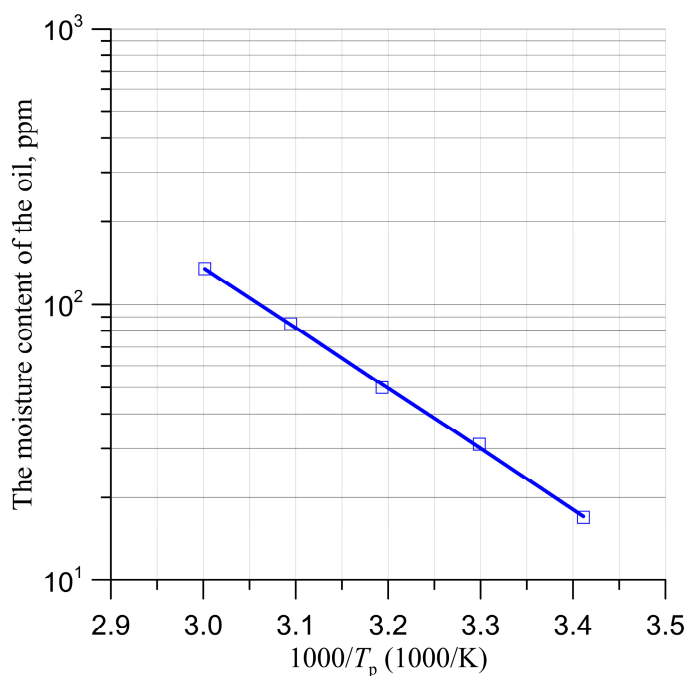
Based on Formula (13), the so-called Arrhenius plot can be made in which the variables  $x = \frac{1000}{T}$  and  $y = \log \sigma$  are used for linearization. In case of a constant value of the activation energy of conductivity, the Arrhenius plot decreases in a straight line.

Figure 7 shows Arrhenius plots for brand new and moistened oil. The graphs were made for the conductivity values measured at the frequency of  $10^{-4}$  Hz (before the first growth stage) and at 1 Hz (after the first growth stage). The figure shows the linear approximations of the experimental results with solid lines. The determination coefficients  $R^2$  values prove the good quality of the approximation. Their values are close to one, and they are 0.9764 and 0.9753 for brand new oil and 0.9967 and 0.9878 for moist oil. For brand new oil, the activation energy values are  $\Delta E(10^{-4} \text{ Hz}) = 0.492 \text{ eV}$  and  $\Delta E(1 \text{ Hz}) = 0.439 \text{ eV}$ . The mean value is  $\Delta E \approx 0.466 \pm 0.0265 \text{ eV}$ . The difference between these values is approximately 5.7%. Oil moisturization causes almost double the increase in activation energy for both frequencies to the values of  $\Delta E_W(10^{-4} \text{ Hz}) = 0.901 \text{ eV}$  and  $\Delta E(1 \text{ Hz}) = 0.878 \text{ eV}$ , respectively, and the mean value of  $\Delta E_W \approx 0.890 \pm 0.0115 \text{ eV}$ . The difference in this case is only 1.3%. The observed increase in the activation energy of conductivity is caused by an increase in the oil water content due to the moistening process. Activation energy increase is related to the increase of the oil moisture level in the state of thermodynamic equilibrium, determined on the basis of the Oommen characteristics [12].



**Figure 7.** AC conductivity Arrhenius plots of mineral-insulating oil with a moisture content of 5 ppm—(a) and moistened mineral oil—(b) at temperatures from 293.15 K to 333.15 K in steps of 8 K for measuring frequencies of  $10^{-4}$  Hz (1) and 1 Hz (2).

On the basis of the Oommen characteristics, the water content of the oil was determined, corresponding to the water content of 5% by weight in the pressboard, for temperatures from 293.15 K to 333.15 K. On this basis, the Arrhenius plot, shown in Figure 8, was made. It can be seen from the figure that the approximation of the data points read from the Oommen characteristics is a decreasing straight line, the coefficient of determination for which is very close to one and amounts to 0.9994.



**Figure 8.** Arrhenius plot for the dependence of the moisture content of the oil in the state of thermodynamic equilibrium between the oil and the pressboard with a moisture content of 5.0% by weight.

The activation energy value of moisture diffusion from the pressboard into the oil determined from the Arrhenius plot is 0.438 eV. In work [12], it was assumed that the state of thermodynamic equilibrium was achieved by the diffusion of water molecules from the pressboard into the oil with the increasing temperature. The diffusion processes are determined by the diffusion coefficient. According to [62], the diffusion coefficient can be defined as:

$$D(T) = D_0 \exp\left(-\frac{\Delta E_D}{kT}\right), \quad (14)$$

where:  $D(T)$ —diffusion coefficient,  $D_0$ —numerical factor,  $\Delta E_D$ —diffusion activation energy,  $k$ —Boltzmann's constant and  $T$ —temperature.

In the case of dielectrics, the conductivity depends on the concentration of places from which the charges involved in current conducting can be released [61]. They are released by thermal activation. Participation in current conduction is determined by the activation energy of migration. This means that, in Formula (13), for conductivity, the activation energy of the conductivity  $\Delta E_\sigma$  is the sum of the thermal activation energy and the migration activation energy. In the case of oil moistening by the diffusion of water from the pressboard, the concentration of water molecules in the oil increases with the temperature proportional to the diffusion coefficient described by Formula (14). This means that the formula for conductivity in the case of water diffusion from the pressboard into the oil should be written as:

$$\sigma_W(T) = \sigma_{W0} \exp\left(-\frac{\Delta E_\sigma + \Delta E_D}{kT}\right), \quad (15)$$

where:  $\sigma_{W0}$ —numerical factor,  $\Delta E_\sigma$ —conductivity activation energy of brand new oil and  $\Delta E_D$ —activation energy of water molecules diffusion from the pressboard into the oil.

The comparative analysis of the electrical properties of brand new and moistened oil shows that the moistening process, which takes place in power transformers, causes an increase in the oil activation energy of conductivity compared to the oil to which no additional moisture is supplied. The comparison of the Arrhenius plots (Figure 7) shows that the activation energy of conductivity increases from the value for the brand new oil

$\Delta E \approx 0.466 \pm 0.0265$  eV to the value for the oil moistened by moisture diffusion from the pressboard  $\Delta E_W \approx 0.890 \pm 0.0115$  eV. The increase in the activation energy of the conductivity due to moisturization is approximately 0.424 eV. The activation energy of water molecules diffusion from the pressboard into the oil, determined from the Arrhenius plot, is 0.438 eV. This is very close to the value of the increase in the activation energy of conductivity caused by moisturization. The difference between them is around 3.2%. The same, within the uncertainty limits, values of activation energy may mean that the increase in the activation energy of the conductivity observed in the moist oil is caused by the diffusion of water molecules from the pressboard into the oil.

#### 4. Conclusions

The study presents measurements of frequency and temperature dependencies of admittance  $Y$ , phase shift angle  $\varphi$ , AC conductivity  $\sigma_{AC}$ , permittivity  $\epsilon'$  and loss tangent  $\tan\delta$  for brand new and moistened oil. The moisturization was done in a manner identical to the oil moistening in power transformers. To do so, pressboard plates with a moisture content of 5% by weight were placed in a vessel with brand new oil. The volume of the pressboard was 10 times smaller than volume of the oil. Moistening was achieved by the migration of moisture from the moistened pressboard into the oil.

It was found that all measured AC electrical parameters of the oil after moistening showed some changes.

Admittance studies have shown that the oil moistening reduces the dielectric relaxation time by about ten times. As the temperature increases, the differences in admittance values for the lowest frequency of  $10^{-4}$  Hz increase. For brand new oil, the change is about 10 times, and, for moisturized oil, about 100 times.

It was found that, in the moistened oil, the section in which the values of the angle  $\varphi$  are close to zero is lengthened. In the area of higher frequencies, the rate of the phase shift angle module increases, and the influence of temperature on the curves shift to the area of higher frequencies, related to the reduction of the dielectric relaxation time value, increases.

It was observed that the permittivity of both brand new and moistened oil in the frequency range above 0.1 Hz is a constant value of about 2.2. Slight changes in permittivity due to moisturization occur in the frequency region below 0.1 Hz.

It was found that moisturization increases the value of  $\tan\delta$  at the frequency of  $10^{-4}$  Hz from about 20 to about 70. The increase in frequency causes a decrease in the value of  $\tan\delta$ . In the frequency area above 10 Hz for brand new oil, a slowing down of the curve decrease is observed, and at a frequency of about 1000 Hz, the minimum is observed. The minimum value is approximately  $4 \times 10^{-4}$ . In the curve for moistened oil, the reduction of the  $\tan\delta$  value occurs faster than for a brand new oil. The minimum for moistened oil occurs at a frequency of about 400 Hz, and its value is about six times lower than for a brand new one. Moreover, the shape of the minimum is very clear compared to the plot for brand new oil. As the temperature increases, the  $\tan\delta$  curves for the moistened oil shift to the higher frequency area much faster than for the brand new oil. It is related to the reduction of the relaxation time due to the increase in moisture.

Brand new oil has two electric current conduction mechanisms. The first occurs at frequencies lower than about 0.01 Hz, the second above 10 Hz. Moistening the oil causes the first segment of an increase in conductivity to disappear. In the second, the rate of conductivity increases. The activation energy of conductivity for the brand new oil— $\Delta E \approx 0.466 \pm 0.0265$  eV—and for the moistened oil— $\Delta E_W \approx 0.890 \pm 0.0115$  eV—was determined from the Arrhenius plots.

The increase in the activation energy of conductivity during oil moistening is caused by the diffusion of water molecules from the pressboard into the oil.

The observed changes in the oil parameters caused by moistening should be taken into account while analyzing the power transformer insulation condition using the FDS method.

In further research, the authors plan to significantly expand their scope. Parameters such as the time to reach thermodynamic equilibrium, their dependence on the moisture content in the pressboard, temperature and a number of others will be determined.

**Author Contributions:** Conceptualization, K.K. and P.R.; methodology, K.K., P.R., V.B., P.O. and D.K.; software, V.B. and P.O.; validation, K.K. and P.R.; formal analysis, K.K., P.R., V.B., P.O. and D.K.; investigation, P.R., V.B., P.O. and D.K.; resources, K.K., V.B. and D.K.; data curation, V.B. and P.O.; writing—original draft preparation, K.K. and P.R.; writing—review and editing, K.K. and P.R.; visualization, V.B. and P.O.; supervision, K.K. and funding acquisition, K.K., P.R., V.B. and P.O. All authors have read and agreed to the published version of the manuscript.

**Funding:** The research was supported by the subsidy of the Ministry of Education and Science (Poland) for the Lublin University of Technology as funds allocated for scientific activities in the scientific discipline of Automation, Electronics and Electrical Engineering—grants: FD-20/EE-2/701, FD-20/EE-2/702, FD-20/EE-2/705 and FD-20/EE-2/707.

**Data Availability Statement:** Not applicable.

**Conflicts of Interest:** The authors declare no conflict of interest.

## References

1. Liao, R.; Hao, J.; Chen, G.; Ma, Z.; Yang, L. A comparative study of physicochemical, dielectric and thermal properties of pressboard insulation impregnated with natural ester and mineral oil. *IEEE Trans. Dielectr. Electr. Insul.* **2011**, *18*, 1626–1637. [[CrossRef](#)]
2. Rouse, T.O. Mineral insulating oil in transformers. *IEEE Electr. Insul. Mag.* **1998**, *14*, 6–16. [[CrossRef](#)]
3. Yang, L.; Liao, R.; Caixin, S.; Zhu, M. Influence of vegetable oil on the thermal aging of transformer paper and its mechanism. *IEEE Trans. Dielectr. Electr. Insul.* **2011**, *18*, 692–700. [[CrossRef](#)]
4. Abderrazzaq, M.H.; Hijazi, F. Impact of multi-filtration process on the properties of olive oil as a liquid dielectric. *IEEE Trans. Dielectr. Electr. Insul.* **2012**, *19*, 1673–1680. [[CrossRef](#)]
5. *Partial Discharges in Transformers*; Working Group D1.29, No 676; IEEE PES Transformers Committee: Piscataway, NJ, USA, 2017.
6. Fabre, J.; Pichon, A. *Deteriorating Processes and Products of Paper in Oil Application to Transformers*; CIGRE: Paris, France, 1960; p. 137.
7. Graczkowski, A.; Gielniak, J. Influence of impregnating liquids on dielectric response of impregnated cellulose insulation. In Proceedings of the IEEE International Conference on Solid Dielectrics-ICSD, Potsdam, Germany, 4–9 July 2010; pp. 513–516.
8. Liu, J.; Zhang, H.; Geng, C.; Fan, X.; Zhang, Y. Aging assessment model of transformer insulation based on furfural indicator under different oil/pressboard ratios and oil change. *IEEE Trans. Dielectr. Electr. Insul.* **2021**, *28*, 1061–1069. [[CrossRef](#)]
9. Pompili, M.; Mazzetti, C.; Bartnikas, R. PD pulse burst characteristics of transformer oils. *IEEE Trans. Power Deliv.* **2006**, *21*, 689–698. [[CrossRef](#)]
10. Pompili, M.; Mazzetti, C.; Forster, E.O. Partial Discharge Distributions in Liquid Dielectrics. *IEEE Trans. Electr. Insul.* **1992**, *27*, 99–105. [[CrossRef](#)]
11. Pompili, M.; Mazzetti, C.; Bartnikas, R. PD pulse burst behavior of a transformer type synthetic organic ester fluid. *IEEE Trans. Dielectr. Electr. Insul.* **2008**, *15*, 1498–1506. [[CrossRef](#)]
12. Oommen, T.V.; Prevost, T.A. Cellulose insulation in oil-filled power transformers: Part II—maintaining insulation integrity and life. *IEEE Electr. Insul. Mag.* **2006**, *22*, 5–14. [[CrossRef](#)]
13. Rahman, M.F.; Nirgude, P. Partial discharge behaviour due to irregular-shaped copper particles in transformer oil with a different moisture content of pressboard barrier under uniform field. *IET Gener. Transm. Distrib.* **2019**, *13*, 5550–5560. [[CrossRef](#)]
14. Hill, J.; Wang, Z.; Liu, Q.; Krause, C.; Wilson, G. Analysing the power transformer temperature limitation for avoidance of bubble formation. *High Volt.* **2019**, *4*, 210–216. [[CrossRef](#)]
15. Garcia, B.; Villarroel, R.; Garcia, D. A Multiphysical model to study moisture dynamics in transformers. *IEEE Trans. Power Deliv.* **2019**, *34*, 1365–1373. [[CrossRef](#)]
16. Martinez, M.; Pleite, J. Improvement of RVM test interpretation using a Debye equivalent circuit. *Energies* **2020**, *13*, 323. [[CrossRef](#)]
17. Islam, M.M.; Lee, G.; Hettiarwate, S.N. A review of condition monitoring techniques and diagnostic tests for lifetime estimation of power transformers. *Electr. Eng.* **2018**, *100*, 581–605. [[CrossRef](#)]
18. Fofana, I.; Hadjadj, Y. Electrical-Based Diagnostic Techniques for Assessing Insulation Condition in Aged Transformers. *Energies* **2016**, *9*, 679. [[CrossRef](#)]
19. Sarkar, S.; Sharma, T.; Baral, A.; Chatterjee, B.; Dey, D.; Chakravorti, S. An expert system approach for transformer insulation diagnosis combining conventional diagnostic tests and PDC, RVM data. *IEEE Trans. Dielectr. Electr. Insul.* **2014**, *21*, 882–891. [[CrossRef](#)]
20. Zheng, H.; Liu, J.; Zhang, Y.; Ma, Y.; Shen, Y.; Zhen, X.; Chen, Z. Effectiveness analysis and temperature effect mechanism on chemical and electrical-based transformer insulation diagnostic parameters obtained from PDC data. *Energies* **2018**, *11*, 146. [[CrossRef](#)]

21. Mishra, D.; Haque, N.; Baral, A.; Chakravorti, S. Assessment of interfacial charge accumulation in oil-paper interface in transformer insulation from polarization-depolarization current measurements. *IEEE Trans. Dielectr. Electr. Insul.* **2017**, *24*, 1665–1673. [CrossRef]
22. Zhang, Y.; Liu, J.; Zheng, H.; Wang, K. Feasibility of a universal approach for temperature correction in frequency domain spectroscopy of transformer insulation. *IEEE Trans. Dielectr. Electr. Insul.* **2018**, *25*, 1766–1773. [CrossRef]
23. Liu, J.; Fan, X.; Zhang, Y.; Zhang, C.; Wang, Z. Aging evaluation and moisture prediction of oil-immersed cellulose insulation in field transformer using frequency domain spectroscopy and aging kinetics model. *Cellulose* **2020**, *27*, 7175–7189. [CrossRef]
24. Yang, L.; Chen, J.; Gao, J.; Zheng, H.; Li, Y. Accelerating frequency domain dielectric spectroscopy measurements on insulation of transformers through system identification. *IET Sci. Meas. Technol.* **2018**, *12*, 247–254. [CrossRef]
25. Kołtunowicz, T.N.; Kierczynski, K.; Okal, P.; Patryń, A.; Gutten, M. Diagnostics on the Basis of the Frequency-Temperature Dependences of the Loss Angle Tangent of Heavily Moistured Oil-Impregnated Pressboard. *Energies* **2022**, *15*, 2924. [CrossRef]
26. Zukowski, P.; Rogalski, P.; Bondariev, V.; Sebok, M. Diagnostics of High Water Content Paper-Oil Transformer Insulation Based on the Temperature and Frequency Dependencies of the Loss Tangent. *Energies* **2022**, *15*, 2813. [CrossRef]
27. Jonscher, A.K. *Dielectric Relaxation in Solids*; Chelsea Dielectrics Press: London, UK, 1983.
28. Cole, K.S.; Cole, R.H. Dispersion and Absorption in Dielectrics II. Direct Current Characteristics. *J. Chem. Phys.* **1942**, *10*, 98–105. [CrossRef]
29. Cole, K.S.; Cole, R.H. Dispersion and Absorption in Dielectrics I. Alternating Current Characteristics. *J. Chem. Phys.* **1941**, *9*, 341–351. [CrossRef]
30. Davidson, D.W.; Cole, R.H. Dielectric relaxation in glycerol, propylene glycol, and n-propanol. *J. Chem. Phys.* **1951**, *19*, 1484–1490. [CrossRef]
31. Davidson, D.W. Dielectric relaxation in liquids: I. The representation of relaxation behavior. *Can. J. Chem.* **1961**, *39*, 571–594. [CrossRef]
32. Havriliak, S.J.; Havriliak, S.J. *Dielectric and Mechanical Relaxation in Materials. Analysis, Interpretation and Application to Polymers*; Hanser Publisher: Munich, Germany, 1997.
33. Zukowski, P.; Rogalski, P.; Kołtunowicz, T.N.; Kierczynski, K.; Bondariev, V. Precise measurements of the temperature-frequency dependence of the conductivity of cellulose—Insulating oil—Water nanoparticles composite. *Energies* **2020**, *14*, 32. [CrossRef]
34. Żukowski, P.; Kierczyński, K.; Kołtunowicz, T.N.N.; Rogalski, P.; Subocz, J. Application of elements of quantum mechanics in analysing AC conductivity and determining the dimensions of water nanodrops in the composite of cellulose and mineral oil. *Cellulose* **2019**, *26*, 2969–2985. [CrossRef]
35. Żukowski, P.; Kołtunowicz, T.N.; Kierczyński, K.; Subocz, J.; Szrot, M. Formation of water nanodrops in cellulose impregnated with insulating oil. *Cellulose* **2015**, *22*, 861–866. [CrossRef]
36. Kołtunowicz, T.N.; Fedotova, J.A.; Zhukowski, P.; Saad, A.; Fedotov, A.; Kasiuk, J.V.; Larkin, A. V Negative capacitance in (FeCoZr)–(PZT) nanocomposite films. *J. Phys. D. Appl. Phys.* **2013**, *46*, 125304. [CrossRef]
37. Zukowski, P.; Kołtunowicz, T.; Partyka, J.; Węgierek, P.; Kolasik, M.; Larkin, A.V.; Fedotova, J.A.; Fedotov, A.K.; Komarov, F.F.; Vlasukova, L.A. Model przewodności skokowej i jego weryfikacja dla nanostruktur wytwarzanych technikami jonowymi. *Prz. Elektrotechniczny* **2008**, *84*, 247–249.
38. Kołtunowicz, T.N.; Zukowski, P.; Boiko, O.; Czarnacka, K.; Bondariev, V.; Saad, A.; Larkin, A.V.; Fedotov, A.K. Capacitive properties of nanocomposite (FeCoZr)<sub>x</sub>(PZT)(100–x) produced by sputtering with the use of argon and oxygen ions beam. *J. Mater. Sci. Mater. Electron.* **2016**, *27*, 1171–1176. [CrossRef]
39. Zukowski, P.; Kołtunowicz, T.; Partyka, J.; Węgierek, P.; Komarov, F.F.; Mironov, A.M.; Butkiewith, N.; Freik, D. Dielectric properties and model of hopping conductivity of GaAs irradiated by H<sup>+</sup> ions. *Vacuum* **2007**, *81*, 1137–1140. [CrossRef]
40. Svitov, I.; Fedotova, J.A.; Milosavljević, M.; Zhukowski, P.; Kołtunowicz, T.N.; Saad, A.; Kierczynski, K.; Fedotov, A.K. Influence of sputtering atmosphere on hopping conductance in granular nanocomposite (FeCoZr)<sub>x</sub>(Al<sub>2</sub>O<sub>3</sub>)<sub>1-x</sub> films. *J. Alloy. Compd.* **2014**, *615*, S344–S347. [CrossRef]
41. Kołtunowicz, T.N.; Zhukowski, P.; Fedotova, V.V.; Saad, A.M.; Fedotov, A.K. Hopping conductance in nanocomposites (Fe<sub>0.45</sub>Co<sub>0.45</sub>Zr<sub>0.10</sub>)<sub>x</sub>(Al<sub>2</sub>O<sub>3</sub>)<sub>1-x</sub> manufactured by ion-beam sputtering of complex target in Ar+O<sub>2</sub> ambient gas. *Acta Phys. Pol. A* **2011**, *120*, 39–42. [CrossRef]
42. Żukowski, P.; Kołtunowicz, T.; Partyka, J.; Fedotova, Y.A.; Larkin, A.V. Hopping conductivity of metal-dielectric nanocomposites produced by means of magnetron sputtering with the application of oxygen and argon ions. *Vacuum* **2009**, *83*, S280–S283. [CrossRef]
43. Kołtunowicz, T.N.; Zhukowski, P.; Fedotov, A.K.; Larkin, A.V.; Patryń, A.; Andryevskyy, B.; Saad, A.; Fedotova, J.A.F.V.V. Hopping conductivity of metal-dielectriype on negative capacitance effect in nanogranular composite films FeCoZr-insulator. *Elektron. ir Elektrotehnika* **2013**, *19*, 37–40.
44. Żukowski, P.W.; Kantorow, S.B.; Kiszczałk, K.; Maciąka, D.; Rodzik, A.; Stelmakh, V.F.; Czarnecka-Such, E. Study of the Dielectric Function of Silicon Irradiated with a Large Dose of Neutrons. *Phys. Status Solidi* **1991**, *128*, K117–K121. [CrossRef]
45. Zukowski, P.W.W.; Rodzik, A.; Shostak, Y.A.A. Dielectric constant and ac conductivity of semi-insulating Cd<sub>1-x</sub>Mn<sub>x</sub>Te semiconductors. *Semiconductors* **1997**, *31*, 610–614. [CrossRef]
46. Zukowski, P.; Rogalski, P.; Kierczynski, K.; Kołtunowicz, T.N. Precise Measurements of the Temperature Influence on the Complex Permittivity of Power Transformers Moistened Paper-Oil Insulation. *Energies* **2021**, *14*, 5802. [CrossRef]

47. Kunicki, M. Experience in exploitation and diagnostics of high voltage transformers fleet. In Proceedings of the 21st IEEE International Conference on Environment and Electrical Engineering and 2021 IEEE Industrial and Commercial Power Systems Europe, Bari, Italy, 7–10 September 2021.
48. Brncal, P.; Gutten, M. Diagnostics of Insulating Condition of Traction Transformer by Frequency Method. *Transp. Res. Procedia* **2021**, *55*, 977–982. [CrossRef]
49. Group, C.W. *Life management Techniques for Power Transformers*; CIGRE: Paris, France, 2003.
50. Landau, L.D.; Lifshitz, E.M.; Pitaevskiĭ, L.P. *Electrodynamics of Continuous Media*; Butterworth-Heinemann: Oxford, UK, 1984.
51. Waygood, A. *An Introduction to Electrical Science*, 2nd ed.; Taylor & Francis Group: New York, NY, USA, 2019.
52. Halliday, D.; Resnick, R. *Physics, Part II*; John Wiley & Sons: New York, NY, USA, 1978.
53. Zhang, M.; Liu, J.; Jia, H.; Chen, Q.; Lv, J.; Chen, X. Modelling the low-frequency electrode dielectric response based on transformer equivalent oil-paper insulation model. *IET Sci. Meas. Technol.* **2019**, *13*, 700–707. [CrossRef]
54. Dervos, C.T.; Paraskevas, C.D.; Skafidas, P.D.; Vassiliou, P. A Complex Permittivity Based Sensor for the Electrical Characterization of High-Voltage Transformer Oils. *Sensors* **2005**, *5*, 302–316. [CrossRef]
55. Zhang, M.; Liu, J.; Lv, J.; Chen, Q.; Qi, P.; Sun, Y.; Jia, H.; Chen, X. Improved method for measuring moisture content of mineral-oil-impregnated cellulose pressboard based on dielectric response. *Cellulose* **2018**, *25*, 5611–5622. [CrossRef]
56. Rogalski, P. Measurement Stand, Method and Results of Composite Electrotechnical Pressboard-Mineral Oil Electrical Measurements. *Devices Methods Meas.* **2020**, *11*, 187–195. [CrossRef]
57. Zukowski, P.; Kierczynski, K.; Koltunowicz, T.N.; Rogalski, P.; Subocz, J.; Korenciak, D. AC conductivity measurements of liquid-solid insulation of power transformers with high water content. *Measurement* **2020**, *165*, 108194. [CrossRef]
58. Zukowski, P.; Rogalski, P.; Koltunowicz, T.N.; Kierczynski, K.; Subocz, J.; Sebok, M. Influence of temperature on phase shift angle and admittance of moistened composite of cellulose and insulating oil. *Measurement* **2021**, *185*, 110041. [CrossRef]
59. DIRANA-PTM-User-Manual-ENU; Omicron Electronics GmbH: Wien, Austria, 2017. Available online: <https://www.omicronenergy.com/pl/products/dirana/#contactmenu-> (accessed on 16 August 2022).
60. Fofana, I.; Wasserberg, V.; Borsi, H.; Gockenbach, E. Challenge of mixed insulating liquids for use in high-voltage transformers, Part 1: Investigation of mixed liquids. *IEEE Electr. Insul. Mag.* **2002**, *18*, 18–31. [CrossRef]
61. Mott, N.F.; Davis, E.A. *Electronic Processes in Non-Crystalline Materials*, 2nd ed.; Clarendon Press: Oxford, UK; New York, NY, USA, 1979.
62. Ladd, M. *Bonding, Structure and Solid-State Chemistry*; Oxford Academic: Oxford, UK, 2016.